Annu. Rev. Phys. Chem. 2023.74:99-121. Downloaded from www.annualreviews.org
Access provided by State University of New York - Stony Brook on 10/24/23. See copyright for approved use.

ANNUAL REVIEWS

Annual Review of Physical Chemistry

Spectroscopic Studies of Clusters of Atmospheric Relevance

Nicoline C. Frederiks, Annapoorani Hariharan, and Christopher J. Johnson

Department of Chemistry, Stony Brook University, Stony Brook, New York, USA; email: chris.johnson@stonybrook.edu

ANNUAL REVIEWS CONNECT

www.annualreviews.org

- Download figures
- Navigate cited references
- Keyword search
- Explore related articles
- Share via email or social media

Annu. Rev. Phys. Chem. 2023. 74:99–121

First published as a Review in Advance on January 25, 2023

The *Annual Review of Physical Chemistry* is online at physchem.annualreviews.org

https://doi.org/10.1146/annurev-physchem-062322-041503

Copyright © 2023 by the author(s). This work is licensed under a Creative Commons Attribution 4.0 International License, which permits unrestricted use, distribution, and reproduction in any medium, provided the original author and source are credited. See credit lines of images or other third-party material in this article for license information.

OPEN ACCESS CC BY

Keywords

atmospheric aerosols, clusters, new particle formation, spectroscopy, climate

Abstract

Atmospheric aerosols exert a significant but highly uncertain effect on the global climate, and roughly half of these particles originate as small clusters formed by collisions between atmospheric trace vapors. These particles typically consist of acids, bases, and water, stabilized by salt bridge formation and a network of strong hydrogen bonds. We review spectroscopic studies of this process, focusing on the clusters likely to be involved in the first steps of particle formation and the intermolecular interactions governing their stability. These studies typically focus on determining structure and stability and have shown that acid-base chemistry in the cluster may violate chemical intuition derived from solution-phase behavior and that hydration of these clusters is likely to be complex to describe. We also suggest fruitful areas for extension of these studies and alternative spectroscopic techniques that have not yet been applied to this problem.

Annu. Rev. Phys. Chem. 2023.74:99-121. Downloaded from www.annualreviews.org
Access provided by State University of New York - Stony Brook on 10/24/23. See copyright for approved use.

1. INTRODUCTION

1.1. Particles in the Atmosphere

CCN: cloud condensation nuclei

IN: ice nuclei

Primary particle: particle emitted into the atmosphere in the particle state

Secondary particle: particle formed in the atmosphere from trace vapor

HB: hydrogen bond

Atmospheric particles play a major role in the global climate and have significant health impacts. Ranging in size from subnanometer to tens of micrometers, these particles collectively make up atmospheric aerosol, a suspension of particles in atmospheric gas (1). The warming and cooling effects of aerosol contribute to the largest uncertainties in the anthropogenic radiative forcing estimates of climate models (2). Aerosol reduces global radiative forcing, leading to a net cooling effect, though the uncertainty of this cooling effect has tended to increase with each assessment. Particles also cool the atmosphere by elastically scattering light back into space (aerosol direct effect) or by seeding clouds that increase the planet's albedo (indirect effect). In the latter case, they may serve as either cloud condensation nuclei (CCN) or ice nuclei (IN), leading to water droplets or ice particles. Smaller effects due to the absorption of radiation and heterogeneous reactions on their surfaces also contribute and may be important locally. While significant progress has been made in understanding these effects, a major contributor to the remaining uncertainties is simply developing reliable models for the flux of particles into and out of the atmosphere in both modern and preindustrial times.

Particles vary wildly in composition, shape, and morphology, with a significant dependence of each on its source (3). Primary particles such as dust, soot, and sea spray are an enormous topic of study, but this review focuses primarily on secondary particles, whose formation and growth to climatically relevant sizes inherently involve processes spanning the molecular- to particle-size regime (1 nm to 1 μm) and thus are amenable to cluster chemistry techniques. Cluster models are also used to provide atomistic snapshots into the surface or aqueous structures and dynamics at play in primary particles. It is well known that secondary particle growth is only spontaneous for single-component particle-vapor systems for particles above a critical diameter; below this diameter, stabilization and growth require the invocation of a more complex chemical mechanism (4). Ultimately, this process begins with the formation of a cluster of just two molecules that is stable enough to collect a third (and so on) before simply evaporating back to vapor. The formation and initial growth of such clusters are typically referred to as new particle formation (NPF), and it is at this stage where the direct and quantitative molecular-level structural and dynamic insights provided by cluster spectroscopic studies prove particularly useful.

1.2. New Particle Formation

Efficient particle formation requires the stabilization of clusters of a few molecules upon forming adducts with incoming vapors. These stable clusters may then grow by uptake of further vapors, coagulate with one another, be absorbed by much larger particles, or evaporate (5). While covalent bond formation would certainly be the most efficient method to achieve cluster stabilization, it seems that this pathway is unlikely. Instead, ionic interactions and hydrogen bonds (HBs) are sufficient to provide enough stabilization to drive NPF. Early stages of NPF appear to be dominated by acid-base clusters, which provide the opportunity to achieve both types of intermolecular interactions. As shown in **Figure 1**, the most plentiful acid and base in the postindustrial atmosphere are sulfuric acid and ammonia, respectively, and these two molecules are sufficient to form and grow new particles (6). However, these two vapors alone form particles too slowly to explain observed NPF rates in the ambient atmosphere, and in certain locations in the present-day atmosphere as well as the preindustrial atmosphere (much less sulfur), sulfuric acid concentrations are too low for this to be the only type of NPF mechanism (7). Extensive work has thus shown that other inorganic acids such as nitric and iodic acids (8, 9), stronger bases such as amines and diamines (10, 11), and highly functionalized organic and biogenic vapors that

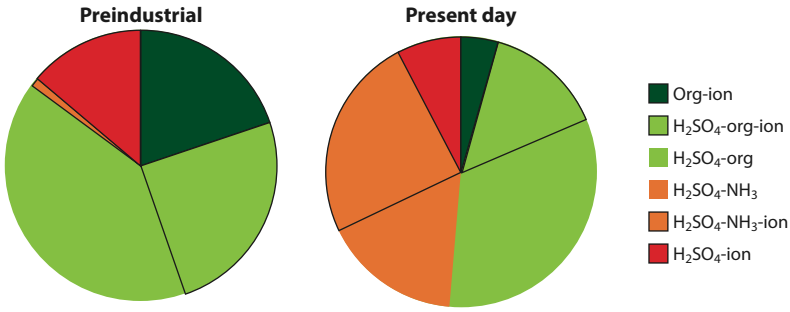

Figure 1

Fraction of newly formed particles by chemical constituents in the preindustrial and present-day atmosphere. Note that the total sulfuric acid concentration in the present-day atmosphere is much higher than that in the preindustrial atmosphere. Figure adapted with permission from Reference 7.

were likely prominent in preindustrial times (7) may play important roles. Importantly, water has been shown to be necessary for particles to form at rates such as those observed in the ambient atmosphere, but the role of water in the NPF mechanism is not well understood (12, 13). While it is crucial for the formation of sulfuric acid from SO_2, it may also play a role in the clusters themselves. Finally, the role of ions has been a matter of discussion for several decades: Ionic clusters are far less plentiful in the atmosphere but may feature faster growth rates at small sizes (14).

2. CURRENT APPROACHES TO STUDYING NEW PARTICLE FORMATION

Given the importance of improving its treatment in climate models, NPF has been the subject of intensive investigation. Ultimately, improved parameterized treatments appropriate for inclusion in climate models are key desired outcomes, but answering fundamental questions about the mechanism of NPF, the molecular species involved, and the atmospheric conditions that promote growth is no less significant. Understanding these aspects of NPF will be necessary to feed back to field studies, to understand the impacts of proposed climate mitigations, and to anticipate how NPF may change with a changing atmosphere. While it is outside the scope of this article, we briefly discuss common methods to study NPF theoretically, in the field, and in the laboratory.

2.1. Theoretical Efforts

Initial efforts to understand NPF focused on classical nucleation theory (CNT), a thermodynamic model that is applicable to spontaneous particle formation processes across chemical species and phases of matter (15, 16). It predicts that a certain critical radius of the particle size must be reached before evaporation of the particle is not thermodynamically favorable compared to growth, typically nanometers to tens of nanometers for systems with a single molecular constituent. CNT assumes, among other things, that newly formed particles feature the same physical properties as the bulk material, an assumption that breaks down at the few-molecule level inherent to the initial steps of NPF. Extensions of CNT have been developed with substantial improvements in accuracy, but the necessity to properly model the first few steps of growth has led to the development of alternate approaches that are atomistic and explicitly account for quantum mechanical interactions such as hydrogen bonding and proton transfer.

A myriad of atomistic approaches have been applied to model NPF, including direct molecular dynamics simulations. The most prolific of these approaches is the atmospheric cluster

Annu. Rev. Phys. Chem. 2023.74:99-121. Downloaded from www.annualreviews.org
Access provided by State University of New York - Stony Brook on 10/24/23. See copyright for approved use.

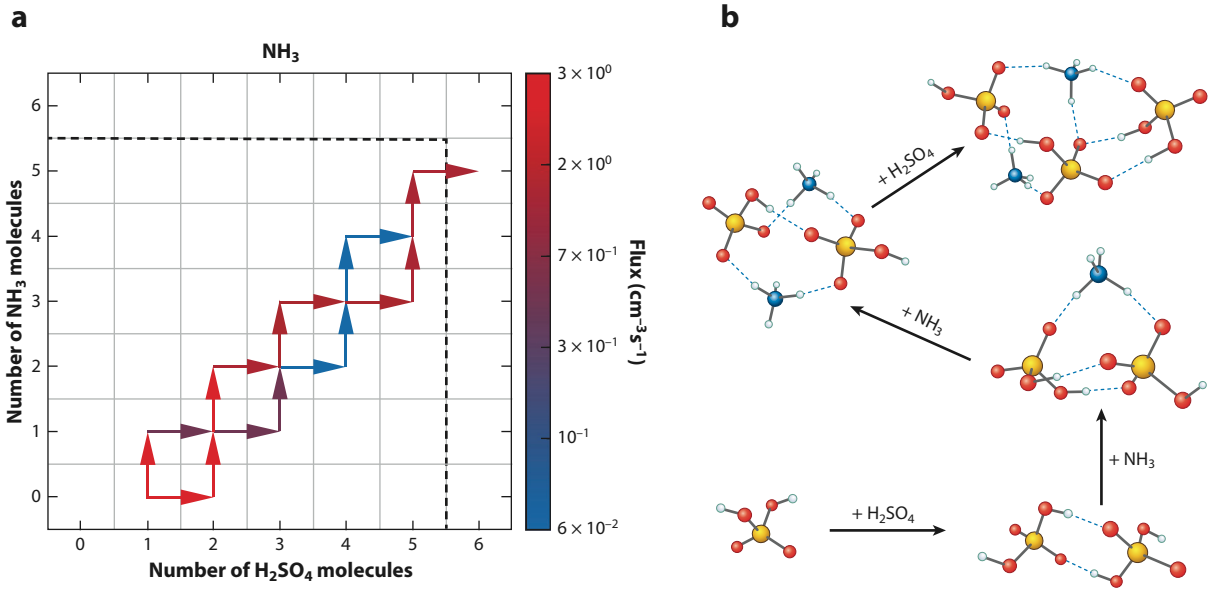

Figure 2

(*a*) The computed growth pathways of clusters of ammonia and sulfuric acid as determined by atmospheric cluster dynamics code (ACDC). (*b*) The structures used for computation of the high-accuracy free energies input into the ACDC simulation in panel *a*. Panel *a* adapted from Reference 10 and panel *b* adapted from Reference 22.

dynamics code (ACDC) (17), which predicts particle formation rates by explicitly computing the rates of growth of clusters molecule by molecule, as depicted in **Figure 2**. This approach requires accurate thermodynamic values for each possible cluster composition, which are usually produced using high-accuracy ab initio quantum chemical calculations (18). ACDC has been successfully used to explore which atmospheric vapors are likely to grow particles at rates similar to those observed in the ambient atmosphere and to model the results of atmospheric simulation experiments in the laboratory, often reproducing experimental results to within an order of magnitude accuracy in the formation rate (19). Some limitations remain, however, including the fact that all clusters are assumed to be in equilibrium at all times and that only one isomer for each cluster composition contributes to growth. While these assumptions are reasonable, given that even relatively fast NPF implies that the addition of individual monomers to the cluster occurs at a rate many orders of magnitude slower than typical molecular timescales, they have not been proven to be true. An additional challenge is the need to find the minimum energy structure for each particle composition (or near enough to it), which is a challenge in any context (20, 21). Many of the studies we discuss in this article directly address cluster structures, providing useful feedback to these efforts. Finally, water is typically treated implicitly in ACDC—if water plays an important role in stabilizing some cluster compositions or isomeric structures over others, this could be an additional source of error.

2.2. Experimental Efforts in the Field

Directly studying NPF in the field is a challenge, given that NPF events do not happen at regular intervals in specific locations, but field studies yield critical real-world information on growth rates, particle compositions, and the conditions required for efficient NPF. For instance, early work correlating particle growth rates with sulfuric acid vapor concentrations showed the centrality of sulfuric acid (23). Broadly speaking, field measurements typically fall into the categories

Annu. Rev. Phys. Chem. 2023.74:99-121. Downloaded from www.annualreviews.org
Access provided by State University of New York - Stony Brook on 10/24/23. See copyright for approved use.

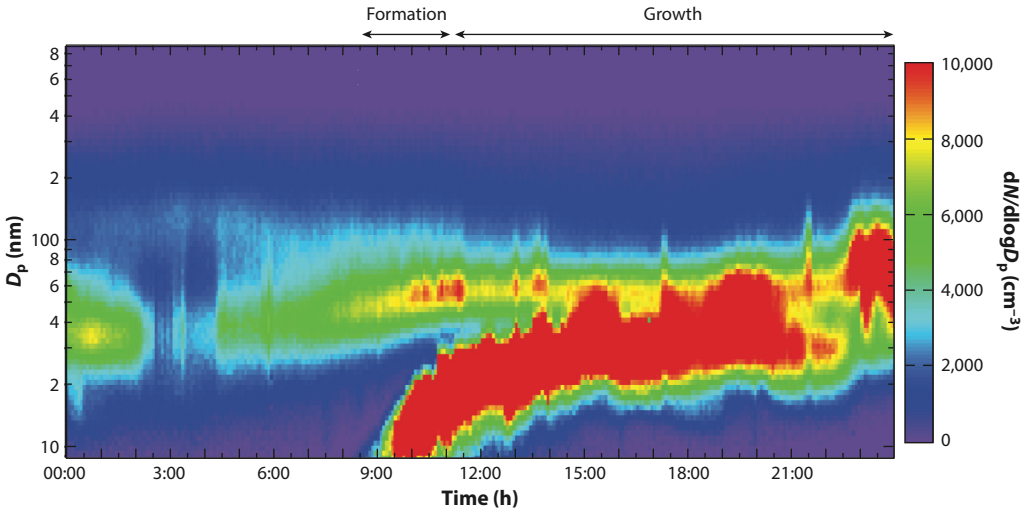

Figure 3

An example of a so-called banana curve in a plot of particle size distribution over time measured during a new particle formation event. Sub-10-nm particles form in the morning and quickly grow to similar sizes as preexisting background particles. Figure adapted with permission from Reference 24.

of particle sizing or mass spectrometry. Sizing instruments have been developed and optimized to measure the concentration of particles as a function of size down to single nanometers and reveal the characteristic so-called banana behavior of NPF, as shown in **Figure 3**. From a roughly constant background of very small particles suddenly arises a burst of new particles that grow rapidly over the course of hours to the size of preexisting particles, either primary or secondary particles that have entered the field of study by transport from their place of birth.

These sizing experiments do not provide the molecular speciation of the particles. For this, mass spectrometry is the primary tool. Starting with early experiments using rockets with a mass spectrometer payload, these experiments have shown the ability to detect molecular clusters in the atmosphere and provide different types of chemical information about their composition (25). In some instruments, new particles are sampled in ambient conditions and vaporized or atomized, yielding information on the atoms or molecules found in ensembles of particles (26, 27). These instruments can be combined with size selection for further specificity. Such experiments have made clear the importance of acids and bases in NPF, but for particles larger than a few nanometers, a myriad of yet-unidentified species are also found to exist in the particles, often making up the bulk of the molecules in the particle (27). Other mass spectrometry experiments focus on minimally activating clusters with the goal of determining their exact compositions. In these instruments, an atmospheric pressure ionization method (often chemical ionization by nitrate or ammonium ions or radiation sources) is used in tandem with a high-resolution, high-accuracy time-of-flight mass spectrometer to determine the exact empirical formulae of clusters (28). Such instruments have been powerful tools to understand particle compositions, but they feature a notable complication: The process of sampling, ionizing, and transporting ambient particles to the vacuum of the mass spectrometer has been shown by careful laboratory experiments to collisionally activate the particles, likely leading to evaporation of some of the particle constituents (29). Determining a priori the extent to which this happens in any given application is likely to be difficult, particularly in the case of water, leading to significant uncertainty in the extent of the hydration of these clusters in ambient conditions.

Annu. Rev. Phys. Chem. 2023.74:99-121. Downloaded from www.annualreviews.org
Access provided by State University of New York - Stony Brook on 10/24/23. See copyright for approved use.

2.3. Experimental Efforts in the Laboratory

Field measurements have the obvious advantage of sampling a realistic atmosphere, but that atmosphere is extremely complex and does not permit straightforward control of conditions or molecular constituents. Laboratory experiments do and can be roughly classified as experiments probing particle formation and growth or isolating and studying the individual clusters themselves. The former often use flow tubes similar to studies of gas-phase atmospheric processes (30) or atmospheric simulation chambers. A prime example of the atmospheric simulation chamber is the Cosmics Leaving Outdoor Droplets (CLOUD) experiment, a multigroup effort to create a large and heavily instrumented chamber (31). CLOUD has leveraged this experimental power to correlate the vapor pressures of specific molecular constituents and atmospheric conditions to both growth rates and cluster compositions using a suite of instruments similar to those discussed in the previous section. This effort has produced benchmark-quality data for comparison to theoretical efforts and has focused other laboratory-based studies (32).

An alternate laboratory-based approach does away with attempts to grow particles in atmospherically relevant conditions and rather obtains clusters from non-native sources. In return for this sacrifice, experiments are able to be conceived that probe clusters of precise composition, allowing the growth process to be probed one molecule at a time. Electrospray ionization (ESI) is one convenient source, and common commercial ESI sources and ESI mass spectrometers (often designed and marketed for biological and medical applications) produce sufficient clusters for study by mass spectrometry. Here relevant acids and bases are dissolved in polar solvents and extruded through a small capillary held at high voltage at atmospheric pressure, producing rapidly evaporating droplets from which clusters emerge. These clusters spend milliseconds or more at atmospheric pressure before being introduced to the vacuum of the mass spectrometer, which could be expected to anneal the initially produced clusters to the most stable compositions. Indeed, we showed that, by optimizing the ESI atmosphere, the distribution of ammonium-bisulfate cations and anions produced by such a source matches nearly exactly that measured in chemical ionization mass spectrometry experiments at CLOUD (33). Coupling alternative measurement techniques such as ion mobility spectrometry to these sources allows for size selection prior to mass spectrometry for additional control over measurements or for initially size-selected clusters to be modified chemically before mass measurement in a tandem arrangement (34).

With these sources in hand, mass spectrometry–based experiments beyond mass measurement can be applied to small particles. Most of these techniques leverage ion traps, which allow precisely mass-selected clusters to be chemically modified and subsequently mass analyzed to determine the effects of these chemical modifications. In ion traps, clusters can be stored under controlled temperature and partial pressures of reactant molecules for specified amounts of time (35). For example, the binding thermodynamics of small sulfuric acid and ammonium-bisulfate clusters can be determined experimentally by storing clusters of initially known composition in an ion trap and monitoring the yield of fragment clusters as a function of trap temperature, yielding kinetic and thermodynamic data (36). Such experiments provide valuable experimental benchmarks for comparison to the quantum chemical efforts described above.

Thus far, our discussion has focused on methods that ultimately identify cluster compositions, but experimental measurements of cluster structures are not possible using these techniques. Thus, theoretical structure searches as discussed above have proceeded largely without experimental support. In this article, we focus on spectroscopic methods that, particularly when combined with relatively simple quantum chemical calculations, permit the exploration of structures. Much of this work leverages the advantage of mass spectrometer–based spectroscopy experiments, wherein individual compositions of clusters can be isolated to yield direct

Annu. Rev. Phys. Chem. 2023.74:99-121. Downloaded from www.annualreviews.org
Access provided by State University of New York - Stony Brook on 10/24/23. See copyright for approved use.

structure-composition relationships, despite not being the only valuable spectroscopic approach that has been employed. We discuss the major questions addressed with these spectroscopy experiments and some future extensions of both experimental methods and NPF-relevant clusters for study.

IRPD: infrared photodissociation

IRMPD: infrared multiphoton dissociation

Cryogenic ion vibrational predissociation spectroscopy (CIVP): considered a subset of infrared photodissociation; also referred to as CIVS

NIPES: negative ion photoelectron spectroscopy

3. SPECTROSCOPY AS AN INDIRECT PROBE OF STRUCTURE

Relatively few experimental methods exist to directly probe the structures of dilute gas-phase objects, particularly mixtures such as those found in the atmosphere. Electron scattering of trapped ions produces scattering patterns that can be compared to simulations based on atomistic models but cannot be directly inverted to structures as in common crystal diffraction experiments (37). Single-particle scattering at X-ray free electron lasers has the potential to fill this role but coupling these user-facility-based experiments to relatively messy samples such as those for sourcing atmospheric clusters requires significant investment (38). Given this, laboratory-scale structural investigations turn to indirect methods, in which spectroscopic observables are compared to quantum chemical predictions of the same observables to determine the best-matching structures.

Two basic spectroscopic techniques have dominated the study of atmospheric clusters: vibrational spectroscopy and electronic spectroscopy. Both harness the power of mass spectrometry to select clusters of exactly known composition for study, allowing the straightforward tracking of structure and properties as a function of size or hydration. Infrared (IR) spectral methods proceed by monitoring the dissociation of the cluster itself [infrared photodissociation (IRPD) or infrared multiphoton dissociation (IRMPD)] (39) or the evaporation of weakly bound adducts (such as N_2) from the surface of the cluster [cryogenic ion vibrational predissociation spectroscopy (CIVP; also known as CIVS) and IRPD] as a function of the wavelength of an IR laser (40). Negative ion photoelectron spectroscopy (NIPES) uses a fixed-wavelength laser with photon energy exceeding the electron affinity of the target anion to photodetach a single electron (41). A NIPES spectrum takes the form of a histogram of the measured binding energy of the emitted photoelectrons, giving insight into the relative energies of the ground and excited states of the anion and corresponding neutral. NIPES can also be used to determine the relative stabilities of compositionally related clusters by formation of an appropriate thermodynamic cycle.

These experiment-theory comparisons are only helpful if the structure probed experimentally is found computationally. For relatively simple clusters, a combination of chemical and spectroscopic intuition is typically sufficient to find an acceptable match. Here, an acceptable match is difficult to define quantitatively; one could be inclined to form a figure of merit, such as the root-mean-squared deviation between the measured and computed spectra, but (particularly for IR spectra) this comparison is complicated by the fact that vibrations dominated by motions of strongly hydrogen-bonded atoms often show large systematic deviations from those predicted by harmonic frequency calculations implemented in typical quantum chemistry software, even for the correct isomer (42). The presence of anharmonic effects not typically accounted for in computed vibrational spectra complicates the picture even further (43, 44). Some of these effects can be ameliorated by the use of molecular dynamics techniques for the computation of vibrational spectra, but at significant additional computational cost. Instead, comparisons are more readily made to shifts of vibrational resonances and splittings in nominally degenerate resonances, which give intuitive information about the hydrogen-bonding environment and symmetry in the cluster and which are better reproduced in quantum chemical calculations.

As an example, we consider the structural elucidation of ammonium-bisulfate clusters, an important class of atmospherically relevant clusters, which has been the focal point of both quantum chemical calculations and laboratory spectroscopy. Studies by Froyd & Lovejoy (36), DePalma

Annu. Rev. Phys. Chem. 2023.74:99-121. Downloaded from www.annualreviews.org
Access provided by State University of New York - Stony Brook on 10/24/23. See copyright for approved use.

Annu. Rev. Phys. Chem. 2023.74:99-121. Downloaded from www.annualreviews.org
Access provided by State University of New York - Stony Brook on 10/24/23. See copyright for approved use.

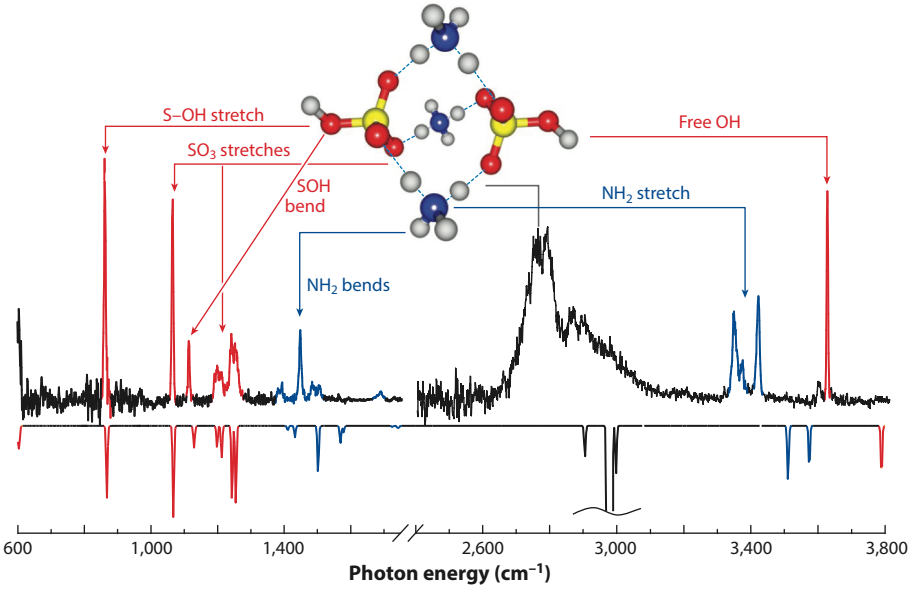

Figure 4

Cryogenic ion vibrational predissociation spectroscopy spectrum of D_2-tagged $(NH_4^+)_3\,(HSO_4^-)_2$, along with (*inset*) a comparison to the calculated spectrum of the apparent minimum-energy structure. Vibrations localized on bisulfate ions are colored in red, while vibrations localized on ammonium ions are blue. Broad intense features from 2,600 to 3,200 cm^{-1} are strongly anharmonically coupled and not well reproduced by harmonic frequency calculations. Figure adapted with permission from Reference 47.

and coworkers (45), and Kupiainen and coworkers (46) found a series of alternate structures. The spectroscopic study of ammonium-bisulfate clusters by Johnson & Johnson (47) on the $(NH_4^+)_3\,(HSO_4^-)_2$ cluster revealed a relatively simple spectrum (shown in **Figure 4**), which features a number of degenerate vibrational resonances supporting the assignment of a highly symmetric structure. Analysis of the spectrum shows a single OH stretching peak, a single S–OH stretching peak, and a single SOH bending peak, suggesting that both bisulfate OH moieties are identical. It also features two sharp NH stretching peaks, typical of symmetric and asymmetric (or antisymmetric) stretching vibrations. Again, the fact that these features are so sharp indicates that all three ammonium ions are in identical arrangements. This pattern is consistent with the highly symmetric structure proposed by Froyd & Lovejoy, and quantum chemical calculations of the vibrational spectrum (bottom of **Figure 4**) confirm the structure of the $(NH_4^+)_3\,(HSO_4^-)_2$ cluster present in the experiment (presumed to be the minimum energy structure given the low-temperature conditions under which the spectrum was recorded) from the pool of previously proposed structures.

Kreinbihl et al. (48) further identified the lowest-energy structures of the $(NH_4^+)_2\,(HSO_4^-)_1$ cluster, but the $(NH_4^+)_4\,(HSO_4^-)_3$ and larger clusters do not yet have a firm assignment. This is discussed further in Section 6. Similarly, the structures of anionic bisulfate–sulfuric acid clusters have been determined using IRMPD spectra with a free electron laser light source, focusing on the fingerprint region of the spectrum, as well as a number of hydrated clusters, as discussed in Section 5.2 (49). Clearly, the determination of the absolute structure using this method is an intensive process that, while valuable, quickly becomes a major challenge. However, as we also discuss, the absolute structure is not necessary to gain structural insights on clusters, given that the telltale spectroscopic responses to changes in structure are understood.

For more complex clusters, the number of candidate structures to produce begins to outstrip the human capacity to produce candidates, and more sophisticated automated approaches must be used. A myriad of computational structure search techniques, developed across multiple fields of research, have been developed to identify global minimum energy structures by combing the potential energy surfaces (PESs) of these clusters (20, 21, 45). Typically, low-cost methods are initially used to broadly search the PESs for different configurations. Promising structure candidates are then subjected to more rigorous, expensive optimization techniques.

Acid strength (pKa): log(fraction of acid dissociated)

Proton affinity (PA): change in free energy upon protonation of an isolated basic site

MA: methylamine

TMA: trimethylamine

DMA: dimethylamine

pKa trend: NH_3 < MA ≲ DMA < TMA

PA trend: NH_3 < MA < DMA < TMA

4. ACID-BASE CHEMISTRY IN CLUSTERS CAN DIFFER FROM THAT IN SOLUTION

Gas-phase molecular interactions fundamentally differ from those in the solution phase, as the solvent effects that support the intuitions chemists have developed are stripped away. Acids and bases with well-known aqueous behavior can interact in unanticipated ways in the gas or cluster phase, and thus ultimately in the atmosphere. Thus, acid strength (pKa) alone cannot fully explain gas-phase acidity/basicity. Gas-phase proton affinity (PA) is a single-molecule property that can also result in inaccurate predictions of proton transfer, because it does not take into account strong mutual interactions arising from, for example, hydrogen bonding and electrostatic interactions with other constituents in a cluster. As a result, the prediction of acid-base chemistry in the gas and cluster phases is not always straightforward, a particular problem for nucleation theories at this size range. As an example, it has been shown that particle formation rates (and, by inference, stability) for sulfuric acid–amine systems follow the trend NH_3 < methylamine (MA) < trimethylamine (TMA) < dimethylamine (DMA), which more closely follows the pKa trend among these amines than the PA trend (30). Presumably, pKa is still representative of some collection of intermolecular interactions, in this case likely the steric hindrance of methyl groups and the number of HBs that can be formed.

4.1. The Strongest Acid May Not Be Deprotonated

One clear example of the violation of solution-phase acid-base rules comes from an IRMPD study on proton transfer in nitrate-bisulfate core clusters (50). In these mixed clusters, the nitrate was found to be the charge carrier instead of bisulfate (**Figure 5**), despite the fact that $(PA)_{nitrate} > (PA)_{bisulfate}$ as well as $(pKa)_{sulfuric\ acid} < (pKa)_{nitric\ acid}$. It is likely that charge delocalization through the formation of HBs factors into the preference of this arrangement. The detection of the nitrate as the charge carrier in this system implies that other cluster systems likely experience comparable proton transfer schemes.

An even more stark example is provided in the anionic sulfuric acid–formate system (51). The presence of two strongly temperature-dependent proton transfer isomers was identified, with the H_2SO_4-$HCOO^-$ isomer being slightly lower in energy compared to the expected HSO_4^--HCOOH isomer despite the pKa of formic acid being more than 10 units higher than that of sulfuric acid. The former (H_2SO_4-$HCOO^-$) is the result of more electron delocalization stabilizing the cluster, since the formate ion binds the proton much less intensely than the bisulfate ion. Further stability is likely the result of two equal strength, strong HBs in the H_2SO_4-$HCOO^-$ isomer compared to the one stronger/one weaker HB of the HSO_4^--HCOOH isomer (**Figure 5**). The lower-energy H_2SO_4-$HCOO^-$ isomer is only dominant at lower temperatures and becomes less prominent with increasing temperature, disappearing completely by ∼300 K. This is likely due to thermal fluctuations interfering in the formation of this isomer as temperature is increased. Similar results have been found in other anionic clusters involving proton transfer from carboxylic acids to sulfuric acid, violating PA and pKa predictions, and thereby establishing a trend in clusters

Annu. Rev. Phys. Chem. 2023.74:99-121. Downloaded from www.annualreviews.org
Access provided by State University of New York - Stony Brook on 10/24/23. See copyright for approved use.

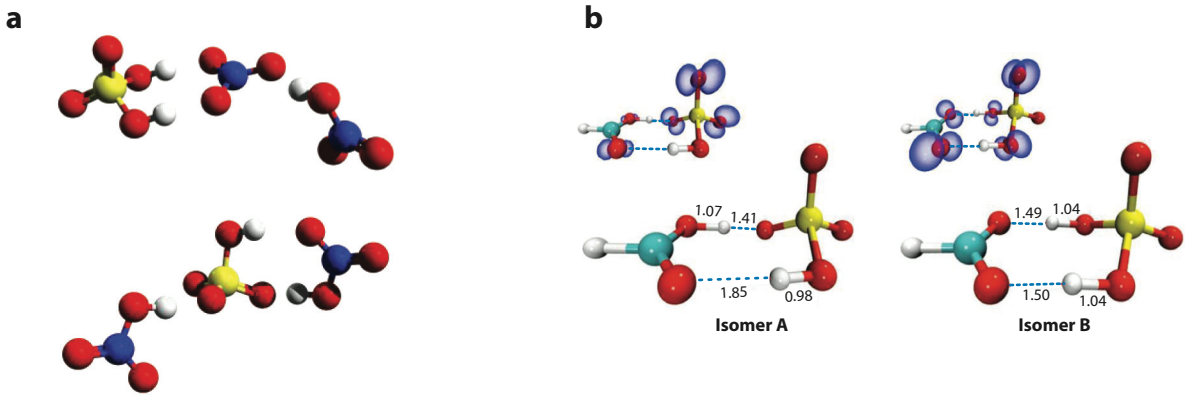

Figure 5

The two lowest-energy structures of (*a*) the deprotonated cluster of sulfuric acid and two nitric acids, and (*b*) the two observed isomers A and B of the H_2SO_4-$HCOO^-$ cluster. In each case, the protonated conjugate base is the opposite of the one expected based on the relative acid strength (pKa) or proton affinities. Panel *a* adapted with permission from Reference 50 and panel *b* adapted with permission from Reference 51.

of this class (51–53). Therefore, strong mutual interactions along with optimal HBs must also be considered when studying these gas clusters.

4.2. Hydrogen Bonding May Prevail Over Acid-Base Chemistry

Organic acids are capable of forming relatively strong HBs with other compounds pivotal in the formation of prenucleation clusters. The formation of short HBs enhances cluster stability while also lowering free energy barriers. Homodimers of dicarboxylic acids with varying aliphatic chain lengths were the focus of one study (54). It was found that the formation of the dimer greatly improves cluster stability (higher binding energies and more negative Gibbs free energy changes) as well as electron stabilization energy, likely due to more delocalization of the negative charge in the dimer due to increased interaction strength. These clusters were found to be stabilized further by an intramolecular O–H···O HB between the carboxylate and carboxylic acid groups in both the monomer and dimer clusters, especially in longer chain-length dicarboxylic acids. The dimer clusters form only one strong intermolecular HB and preserve the two intramolecular HBs. However, the carboxylate component's intramolecular HB was found to become slightly weaker as the carboxylic acid component's intramolecular HB becomes slightly stronger. These intramolecular HBs help stabilize the dimers through increased charge delocalization (54). Similar stabilizing intramolecular HBs were found to be present in succinic acid (SUA)·(HSO_4^-) clusters (53).

The competition between proton transfer and hydrogen bonding was illustrated in cationic ammonium-bisulfate, aminium-bisulfate, and mixed aminium-ammonium-bisulfate clusters via CIVP (55). The amines studied here include MA, DMA, and TMA. Beyond their impacts on particle growth rates, amines are a convenient way to probe HB donor sites, as they directly regulate available HB donors. As shown in **Figure 6** for the $(NH_4^+)_3$ $(HSO_4^-)_2$-, $(MA^+)_3$ $(HSO_4^-)_2$-, and $(DMA^+)_3$ $(HSO_4^-)_2$-containing clusters, each conjugate acid component forms one N–H···O–S HB to each conjugate base, thereby bridging the bisulfate moieties. Since this arrangement cannot be preserved in the TMA-containing cluster, as it only has one HB donor available per TMA molecule, the $(TMA^+)_3$ $(HSO_4^-)_2$ cluster results in fewer HBs formed between the acid and base components. The formation of a single N–H···O–S HB to a single HSO_4^- entity ensues, as well

SUA: succinic acid

Annu. Rev. Phys. Chem. 2023.74:99-121. Downloaded from www.annualreviews.org
Access provided by State University of New York - Stony Brook on 10/24/23. See copyright for approved use.

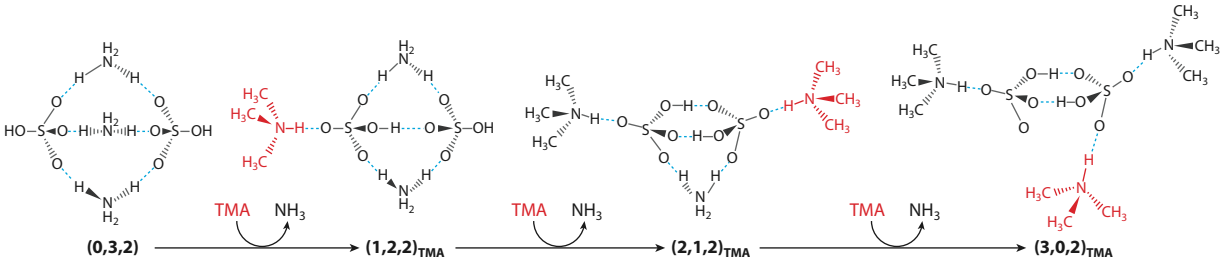

Figure 6

The structural evolution of $(NH_4^+)_3(HSO_4^-)_2$ upon sequential substitution of NH_3 by trimethylamine (TMA). Despite TMA being a much stronger base, the loss of hydrogen-bond donors forces two nominally anionic bisulfate molecules to hydrogen bond with one another, suggesting that hydrogen bonding can outcompete proton transfer to determine the protonation state. Figure adapted with permission from Reference 55.

as the formation of two HBs between the nominally anionic bisulfate moieties, an electrostatically improbable arrangement that has been seen in confined systems (56). Although TMA has the highest PA, the reduction in acid-base HBs lowers the stability of the $(TMA^+)_3(HSO_4^-)_2$ cluster as well as the comparative ability of NPF enhancement via TMA substitution. This study emphasizes the importance of available HB donor sites on cluster stability and suggests that lower-level computational approaches that do not accurately treat hydrogen bonding may miss important structures.

Several carboxylic acid–sulfuric acid clusters have already been discussed; however, one factor we have not addressed is the role functional groups play in these acid-base interactions. Several different volatile organic compound (VOC)-bisulfate clusters have been explored, including α-pinene, alcohols (pinanediol), monocarboxylic acids (*p*-toluic acid, benzoic acid, formic acid, acetic acid, and pentanoic acid), ketone-carboxylic acids [*cis*-pinonic acid (cPA)], dicarboxylic acids (pinic acid, oxalic acid, and SUA), and tricarboxylic acids [3-methyl-1,2,3-butanetricarboxylic acid (MBTCA)]. Depending on the functional group, the preferred charge carrier varies along with the number and strength of HBs between the acid and base moieties. In the case of cPA and *cis*-toluic acid, the VOC was the favored charge carrier by a very small energy margin. In the case of α-pinene, pinanediol, pinic acid, and MBTCA, the charge carrier preferred the bisulfate entity by a narrow energy amount. These findings suggest that proton transfer isomers for these organic–sulfuric acid clusters likely exist together in experiment. For MBTCA and pinic acid, the proton transfer isomer is almost energetically degenerate with the nonproton transfer isomer, so in the case of both di- and tricarboxylic acids the probability of these isomers coexisting is even higher. The linearity of these VOCs also greatly impacts the number of HBs formed between acid-base entities. Planar or more linear VOCs are typically able to form fewer HBs between the HSO_4^-/H_2SO_4 moiety and VOC. In both cPA (linear) and *cis*-toluic acid (planar) clusters, only two HBs are formed in the lowest-energy structure, whereas, in the case of α-pinene, pinanediol, pinic acid, and MBTCA, three intermolecular HBs appear to be energetically favorable, with MBTCA forming an intramolecular HB as well. These more folded/functionalized VOCs are more stable as a result of their increased mutual interaction. In the case of organics, functional groups and the number of HBs play an important role in cluster stability and the identification of key structural interactions (57).

Taken together, these studies show that unintuitive acid-base chemistry is likely at play in dry clusters in the atmosphere. Fortunately, they also suggest that quantum chemical calculations, primarily density functional theory here, appear to reliably model this chemistry. Thus, computational efforts employing such methods are likely to accurately represent the minimum energy

VOC: volatile organic compound

cPA: *cis*-pinonic acid

MBTCA: 3-methyl-1,2,3-butanetricarboxylic acid

Annu. Rev. Phys. Chem. 2023.74:99-121. Downloaded from www.annualreviews.org
Access provided by State University of New York - Stony Brook on 10/24/23. See copyright for approved use.

structures, provided that the relevant structure is sampled during broad structural searches that typically use lower-level quantum chemical or force field methods. It is clear that rationalization of cluster-phase mechanisms must account for the potential of proton-driven chemistry that would be unexpected in solution.

5. CLUSTER HYDRATES TAKE ON COMPLEX STRUCTURAL MOTIFS

Hydration is a difficult aspect of atmospheric clusters to probe, as many experimental methods result in the evaporation of water from the cluster of interest during the sampling process (58–60). Hydration results from the addition of water molecules through hydrogen bonding to the dry cluster or another solvent molecule on the surface of the cluster, meaning we must also understand the competition between solute–solvent effects as well as solvent–solvent effects. Breaking down the hydration of simple monatomic and polyatomic cations and anions can therefore result in the identification of key hydration motifs applicable to these larger atmospherically relevant clusters.

5.1. Hydration Principles of Isolated Ions

Cations and anions typically play different roles in hydration, as summarized in **Figure 7**. Cations tend to act predominantly as HB donors to water, whereas anions typically act as either single or double HB acceptors to water. There have been a handful of studies performed on hydrated cations, including $(Mg^{2+})(H_2O)_{2–10}$, $(H_3O^+)(H_2O)_{1–3}$, and $(NH_4^+)(H_2O)_{3–6}$. For the monatomic cations $(Mg^{2+})(H_2O)_{2–10}$, the Mg^{2+} core is able to interact directly with the oxygens of up to six water molecules (61). In $(H_3O^+)(H_2O)_{1–3}$ and $(NH_4^+)(H_2O)_{3–6}$ studies, the central cation acts as a single HB donor to the incoming water molecules (62, 63). In the more hydrated $(NH_4^+)(H_2O)_{3–6}$, more extensive solvent–solvent hydrogen-bonding interactions persist with additional hydration once each HB donor has preferentially formed at least one HB with an acceptor (62). In the $(I^-)(H_2O)_{1–4}$ anionic system, the I^- prefers to interact with a single hydrogen of each water molecule, and as a result begins to form an interwater HB network starting at two water molecules (64). This is likely due to the nature of the monatomic anionic core, making the interwater HB network sterically more favorable after the addition of a second water molecule.

Several more studies have been performed on polyatomic anionic hydrated systems, including $(NO_3^-)(H_2O)_{n=1–6}$, $(HSO_4^-)(H_2O)_{n=1–16}$, and $(SO_4^{2-})(H_2O)_{n=3–24}$. In both the $(NO_3^-)(H_2O)_{1–6}$ and $(SO_4^{2-})(H_2O)_{1–16}$ systems, the first three and four water molecules, respectively, prefer to form two donor HBs to the anionic core (65–70). In the bisulfate system, the presence of an OH HB donor results in the possibility of the formation of a third HB in the $n = 1$ cluster, in which

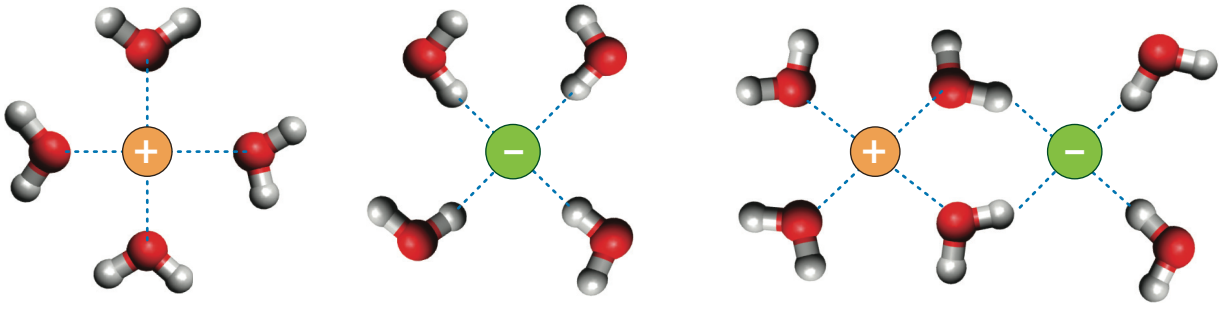

Figure 7

Depiction of the expected hydration motifs of isolated cations, isolated anions, and salt clusters. Bridging water molecules suggest the beginning of solvent-separated ion pair formation as the first step toward dissolution.

Annu. Rev. Phys. Chem. 2023.74:99-121. Downloaded from www.annualreviews.org
Access provided by State University of New York - Stony Brook on 10/24/23. See copyright for approved use.

the water oxygen can act as an HB acceptor from the bisulfate OH. As a result, by the addition of a second water molecule, an interwater HB network can begin to form in the bisulfate system (71). Both studies on $(NO_3^-)(H_2O)_n$ propose that an interwater HB network only starts forming at the $n = 4$ cluster size (65, 67). However, the number of water molecules necessary to form the first solvation shell remains disputed (65, 67). $(SO_4^{2-})(H_2O)_{1–16}$ needs at least three water molecules to exist in a stable form and balance out the two negative charges, but by the $n = 5–6$ cluster size, an interwater HB network can begin to form (68–70). Even though isomers with more water–water HBs were found to be significantly higher in energy ($n = 4–7$), they were still found to exist at room temperature (70). In the $(HSO_4^-)(H_2O)_{1–16}$ system, at $n = 4$, the four water molecules are linked via several HBs to form a ring yet also bind directly to the bisulfate core, beginning the formation of a stable solvation shell. This initial ring is seemingly localized preferentially on the side of the bisulfate containing the OH group. The presence of an HB donor in this anionic core results in less symmetric early hydration of the core, and thus solvent–solvent effects play a more important role in the earlier stages of hydration (71).

The hydration of anionic organic acid clusters has also been explored. The oxidation products of α-pinene, a prevalent biogenically emitted monoterpene, are at the heart of these studies. These oxidation products typically contain hydrophobic hydrocarbon backbones supporting hydrophilic functional groups. For example, cPA^- with up to five water molecules exhibits two potential isomers for the unhydrated cPA^-: a linear structure (**Figure 8*a***) and a folded structure with an intramolecular HB. The lowest-energy isomers for the singly hydrated ion prefer to form two single donor/single acceptor HBs. The addition of water is localized exclusively on the carboxylate group of the cPA^- core, irrespective of the shape of the core. An interwater HB network therefore begins to form by the addition of a second water molecule, much sooner than in the inorganic core clusters. As a result, this organic acid cluster does not appear to form a solvation shell hydration motif surrounding the entire molecule but prefers to exclusively hydrate around the carboxylate group (**Figure 8*a***). Unlike their inorganic counterparts, the hydration of these organic acid clusters is largely dependent upon functional groups (72).

Another study concentrated on the dianionic oxidation product of α-pinene, the *cis*-pinate ion, solvated with up to $n = 4$ water molecules. *Cis*-pinic acid is a rigid dicarboxylic acid, meaning it has more hydrophilic functional groups than cPA, resulting in more potential sites for water to access. Since water can add to each available carboxylate group, the interwater HB network likely does not begin to form until the $n = 3$ cluster size. However, evidence was found that the higher-energy isomer, in which solvation occurred on only one carboxylate group exclusively, is competitive with the equal hydration of both carboxylate groups starting at $n = 3$ (73). A previous study on hydrated flexible dicarboxylate dianions of varying hydrocarbon chain lengths ($m = 2, 4, 8$) found that this class of organic acids preferred to hydrate symmetrically between the two carboxylate groups. The extent of hydration was also found to impact whether the dicarboxylate dianion formed a more folded structure instead of the usual linear shape these acids typically adopt (74).

5.2. Competition Between Intermolecular Interactions in Cluster Hydration

Expanding upon the inorganic anionic systems discussed above, the hydration of clusters containing several core components was explored by Heine et al. (75), who studied nitrate clusters composed of $(NO_3^-)(HNO_3)_m(H_2O)_n(H_2)_z$, where $m = 1–3$, $n = 1–8$, and $z \geq 1$. The shared proton and its response to solvation were the focus of this study. In the unsolvated cluster they found that the nitrate cores essentially share this proton equally through two short, strong HBs. Asymmetric and/or more substantial hydration ($n \geq 1$) weakens this strong HB and results in a complete proton transfer. Comparison of $(NO_3^-)(HNO_3)_2(H_2O)_8$ to a thin film absorption spectrum

Annu. Rev. Phys. Chem. 2023.74:99-121. Downloaded from www.annualreviews.org
Access provided by State University of New York - Stony Brook on 10/24/23. See copyright for approved use.

Annu. Rev. Phys. Chem. 2023.74:99-121. Downloaded from www.annualreviews.org
Access provided by State University of New York - Stony Brook on 10/24/23. See copyright for approved use.

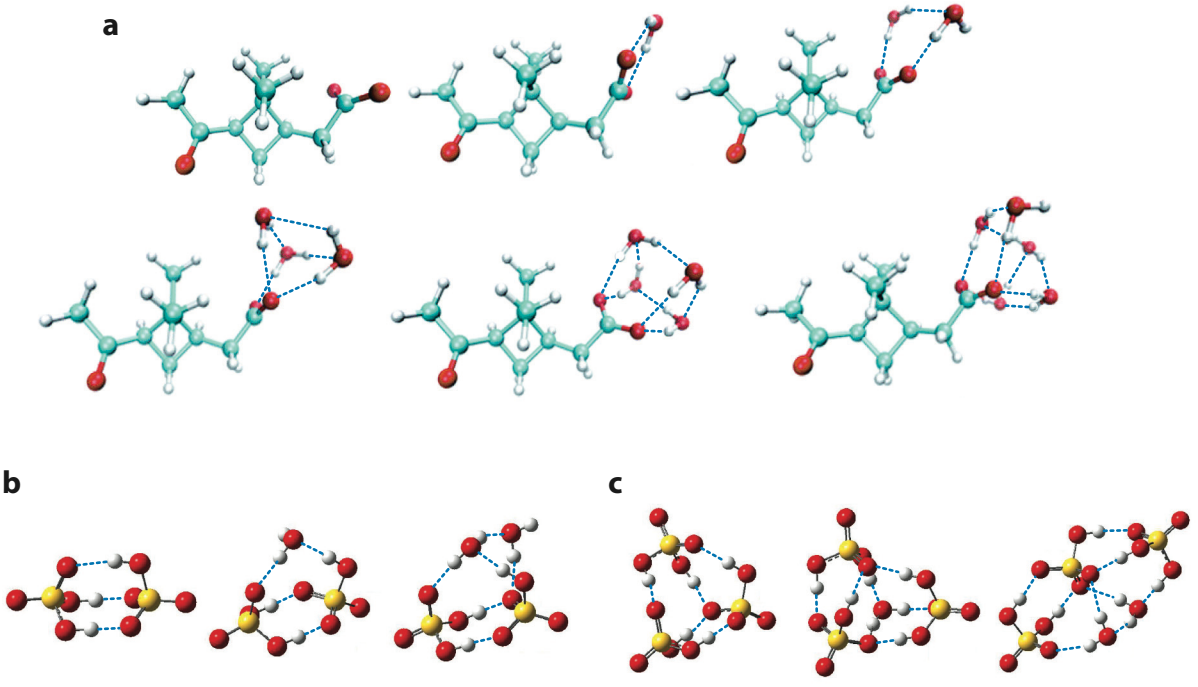

Figure 8

Low-energy structures of (*a*) *cis*-pinonic acid (cPA) $(H_2O)_n$ (isomer A) clusters ($n = 0$–5) (where O is shown in *red*, C in *cyan*, and H in *white*) showing the formation of a water droplet on the carboxylate with increasing hydration, (*b*) $(HSO_4^-)(H_2SO_4)_m(H_2O)_n$ clusters ($m = 1$, $n = 0$–2), and (*c*) $(HSO_4^-)(H_2SO_4)_m(H_2O)_n$ clusters ($m = 2$, $n = 0$–2). Despite the wealth of hydrogen-bonding partners in the sulfuric acid clusters, water molecules appear to prefer water–water hydrogen bonds when possible. Panel *a* adapted with permission from Reference 72; panels *b* and *c* adapted with permission from Reference 49.

of 15% (HNO_3) implies a fully solvated core (75). For the $(HSO_4^-)(H_2SO_4)_m(H_2O)_n(H_2)_z$ system (where $m = 1$–3, $n = 1$–2, and $z = 0$ or ≥ 1) (**Figure 8*b***), in all of the unhydrated clusters, there exists a hydrogen-bonding motif in which the bisulfate forms three HBs to a sulfuric acid. The impact of the addition of water varies as a result of the number of core components. The larger clusters tend to break this triple hydrogen-bonding arrangement in favor of forming HBs between acid components and additional water molecules. The clusters containing only one sulfuric acid with a bisulfate, however, prefer to preserve this triple HB. These findings suggest that the number of unhydrated ion core components significantly impacts the means of accommodation of water molecules into the cluster and therefore likely impacts the magnitude of hydration (49). The extent of hydration in the $(N_2O_5)(Cl^-)(H_2O)$ system also showed that halide substitution prevailed over hydrolysis until sufficient hydration was achieved to outcompete substitution (76). These studies have begun to detect the early stages of the formation of solvent-separated ion pairs (SSIPs).

SSIPs result when a solvent molecule inserts between cationic and anionic constituents, essentially dissolving the salt core (77). However, this is only possible if adequate hydration is achieved; otherwise, the salt core prefers to remain intact and only hydrates via available HB donors and acceptors. With a hydrated ionic pair involving both cationic and anionic components, the cationic species might be expected to interact/hydrogen bond with the oxygen entities

SSIP: solvent-separated ion pair

of the water molecules and the anionic species to interact/hydrogen bond with the hydrogens of the water molecules, more or less equivalently. However, in the overall cationic systems of $[MgNO_3(H_2O)_{1-4}]^+$ and $[(MgSO_4Mg)(H_2O)_{4-11}]^{2+}$, the positively charged Mg^{2+} molecules hydrate more extensively than the anionic components. The anionic components typically end up forming stabilizing HBs once the more abundantly hydrated cationic constituents are sufficiently hydrated (77, 78). With overall anionic charged clusters, such as $(NaSO_4^-)_2(H_2O)_{0-6,8}$, hydration of the anionic component is favored, with little to no interaction with the Na^+ atoms (79). These findings hint at the importance overall cluster charge plays in hydration.

The ammonium-bisulfate clusters discussed above present a variety of HB donor and acceptor moieties. In the $(NH_4^+)_2(HSO_4^-)_1$ cluster, water was found to insert into a weak preexisting HB between an ammonium NH and a bisulfate OS, suggesting that water favors the formation of at least two HBs, one single donor and one single acceptor (80). In the slightly larger $(NH_4^+)_3(HSO_4^-)_2$ cluster, the first water molecule was found to preferentially bind to a free NH group and form a second stabilizing HB to a nearby bisulfate OS, again forming two HBs. Sequentially hydrating the $(NH_4^+)_3(HSO_4^-)_2$ cluster resulted in the additional water molecules forming HBs to other free NH sites and stabilizing HBs to nearby OS groups. By the addition of the fourth water molecule, no free NH sites were available, so the next optimal site was an HB to a free bisulfate OH and a stabilizing HB with a nearby water molecule (81). Similar to previously examined inorganic core clusters, the interwater HB network begins to form by the addition of the fourth water molecule at this cluster size. The $(NH_4^+)_4(HSO_4^-)_3$ cluster spectrum suggested the presence of at least two isomer classes, and an IR–IR hole burning experiment confirmed this. One isomer class was found to contain the same NH–(H)···OH–OS binding motif as the $(NH_4^+)_3(HSO_4^-)_2$ cluster. The second class of isomers had the water molecule form three HBs, one donating to a bisulfate OS and two accepting HBs from an ammonium free NH and a bisulfate free OH, which was slightly lower in energy than the former structure (80).

Finally, we consider whether the degree of hydration of the clusters in these studies is representative of the degree of hydration of these clusters in the atmosphere. Ion mobility cross sections of cationic DMA–sulfuric acid clusters in humid flows showed less than a 10% increase, suggestive of fewer than five bound water molecules (82). This is consistent with the one to three water molecules that our group observed for smaller clusters of the same composition (83). Similarly, the bisulfate–sulfuric acid clusters discussed above were studied with up to two bound water molecules (49), while calculations for the same clusters suggest that these clusters are likely to contain from zero to three water molecules at atmospheric conditions, with a weak dependence on relative humidity (84). While this does not prove that all studies will show relevant hydration, it does suggest that there is a straightforward approach to determining those conditions.

6. LOOKING BEYOND ABSOLUTE STRUCTURES

The studies discussed so far have focused largely on insights gained from deriving the exact structure—the detailed view of the relative orientations of each molecule in the cluster, their protonation state, and their HB linkages. As the cluster size increases past a few nanometers (roughly 10 molecules), this quickly becomes challenging, and efforts will necessarily need to shift to more qualitative spectroscopic analysis to continue to follow particle growth to the CCN/IN stage.

Even for relatively small clusters [for example, the $(NH_4^+)_4(HSO_4^-)_3$ cluster], this becomes apparent. By comparing the peak energies and band patterns between the computed harmonic spectra and the experimentally obtained CIVP spectra, Kreinbihl et al. (48) identified internal bisulfate-bisulfate hydrogen bonding as a source of added stability for this cluster but were unable to unambiguously determine the absolute structure. However, this was found to be the

Annu. Rev. Phys. Chem. 2023.74:99-121. Downloaded from www.annualreviews.org
Access provided by State University of New York - Stony Brook on 10/24/23. See copyright for approved use.

MIIRS: matrix isolation infrared spectroscopy

FTIR: Fourier transform infrared spectroscopy

Decomposition products: CO, CO_2, and H_2O for formic acid; SO_3 and H_2O for sulfuric acid

ATR: attenuated total reflection

Annu. Rev. Phys. Chem. 2023.74:99-121. Downloaded from www.annualreviews.org
Access provided by State University of New York - Stony Brook on 10/24/23. See copyright for approved use.

smallest cationic cluster that bore all of the spectral features of bulk 180-nm ammonium-bisulfate particles, and thus the assignment of its dominant spectroscopic features should allow for the structural motifs present in larger particles to be tracked. The characteristic previously unidentified band at ~1,300 cm^{-1} in bulk ammonium-bisulfate particles corresponds to the out-of-plane O–H bending of a bisulfate-bisulfate bond. Such cluster-scale insights can then be translated to vibrational spectra of larger particles, providing their spectra can be obtained.

As clusters become larger, the utility of exactly identifying the cluster structure is reduced, and more convenient experimental schemes are likely to become very valuable. For instance, matrix isolation infrared spectroscopy (MIIRS) of different atmospherically relevant clusters (85, 86) adds crucial evidence for the general structural motifs in these clusters, despite lacking the ability to isolate or identify specific cluster compositions. Specifically, the series of experiments carried out on systems with different compositions of sulfuric acid, ammonia, amines, and water (embedded as so-called impurities in solid argon matrices) that were studied via Fourier transform infrared spectroscopy (FTIR) have shown that the $H_2SO_4 \cdots NH_3$ interactions are much stronger than the $H_2SO_4 \cdots H_2O$ interactions. The former is strong enough to initiate a complete proton transfer from H_2SO_4 to NH_3, forming the ionic $NH_4^+HSO_4^-$ complex (seen in the gas phase). However, this study also established that in order for cationic clusters to form, there must be more than one acceptor molecule such as NH_3, H_2O, etc. The sensitivity of the bisulfate stretching modes to the hydrogen-bonding environment in a cluster/complex is further evidenced by matrix isolation studies of the TMA/H_2SO_4/H_2O and H_2SO_4/SO_3/H_2O systems (87, 88). While the expected proton transfer between sulfuric acid and TMA was observed, there is no proton transfer in the sulfuric acid/SO_3/H_2O system, with both hydrogen-bonding arrangements being traceable through the bisulfate stretching modes.

MIIRS studies have shown evidence of complex formation between H_2SO_4 (87) and formic acid (89) with their respective decomposition products. On the one hand, these two studies hint at the possibility of atmospherically relevant neutral clusters forming between an acid and its decomposition products in the absence of an N-containing base, while, on the other hand, matrix isolation studies of acetic acid–water systems have established a temperature dependence for the existence of high-energy cyclic isomers that at lower tropospheric temperatures might directly influence the formation of other key components such as SO_3 and glyoxal (90). The structural information obtained on these small clusters has to be translated to larger particles that are on the order of tens of nanometers in diameter, in order to behave as CCN. The molecular-level understanding of atmospheric nanoparticles is currently held back due to the absence of sufficiently sensitive techniques that can characterize mass-/size-selected nanoparticles in the absence of solvent interaction. Traditional absorption spectroscopy can be performed on larger (hundreds of nanometers) particles, either by passing IR light through a flow tube or by depositing particles on an attenuated total reflection (ATR)-FTIR window for subsequent analysis. These experiments were used to monitor the efflorescence and deliquescence of particles by varying the relative humidity (91, 92).

Clusters also serve as convenient laboratories to investigate interfacial and aqueous phenomena of atmospheric relevance. As one example, the interaction of N_2O_5 with halide ions (X^-) in sea spray aerosols is one potential route to create the XNO_2 molecule. Analysis of the IR spectra of clusters of the form $X^- \cdot N_2O_5 \cdot H_2O$ showed a new mechanism in which the direct insertion of X^- into N_2O_5 is possible and increasingly likely as the halide is varied from Cl^- to I^- (93). **Figure 9** shows how the reaction energetics to form the possible products XNO_2 or HNO_2 vary as a function of halide identity. Subsequent ab initio molecular dynamics studies revealed the mechanism for this reaction in detail, showing how this reaction competes with the previously known hydrolysis reaction of the same system (76).

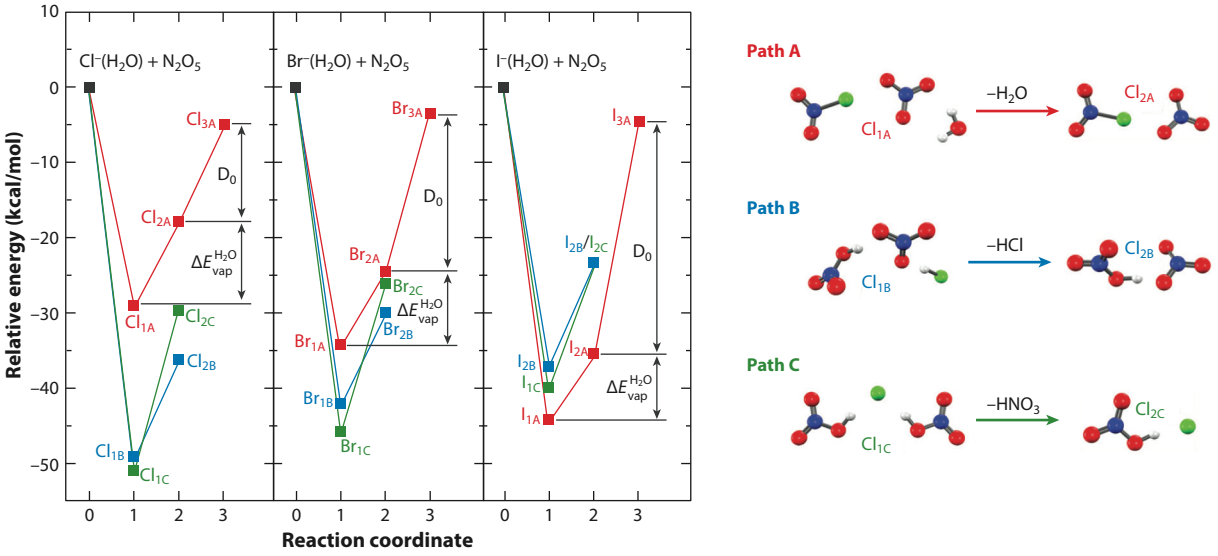

Figure 9

A depiction of the reaction energetics of $X^- \cdot N_2O_5 \cdot H_2O$ for X = Cl, Br, I, as confirmed by vibrational spectra. Insertion (path A) becomes energetically favorable for iodine, presumably because of ion–dipole interactions with the larger INO_2 dipole. Figure adapted with permission from Reference 93.

Electrodynamic balances coupled with mass spectrometry and/or spectroscopy techniques have been used recently to levitate atmospheric nanoparticles to explore the possible reactions contributing to their formation and growth (94, 95). Recent advances in gas-phase mass spectrometry might open new avenues for the study of nanoparticles. The single nanoparticle action spectrometer developed by Esser et al. (96) combines a temperature-controlled (8–350 K) split ring electrode with a mass spectrometer to study ESI-generated single nanoparticles by action spectroscopy. In spite of the greater experimental demand of studying a single particle at a time, it is conceivable that this newly designed instrument can be applied to obtain valuable information on atmospheric nanoparticles.

7. FUTURE PROSPECTS

The results discussed above show the power of cluster spectroscopy techniques to yield insight into atmospheric clusters that is difficult to obtain via typical atmospheric measurement techniques. They also serve as proofs of concept for expanding spectroscopic studies to other aspects of the NPF process or to other atmospherically relevant clusters. Here we take the liberty of proposing future directions for these types of studies or expansions to other experimental techniques that are likely to yield complementary information.

7.1. Expanding the Scope of Vapors Under Study

To date, the bulk of spectroscopic work has focused on sulfuric acid, given its central position to NPF, supporting vapors such as amines and organics, as well as water. Given the relative diversity of structure and functional groups found in organics produced by the oxidation of common vapors such as isoprene and α-pinene, organics certainly deserve additional study. Anecdotally, our lab has struggled to produce clean mass spectra of small clusters containing organics and sulfuric acid or bases. Perhaps this points to a fundamental insight about the size range in which

Annu. Rev. Phys. Chem. 2023.74:99-121. Downloaded from www.annualreviews.org
Access provided by State University of New York - Stony Brook on 10/24/23. See copyright for approved use.

organics contribute to NPF, or perhaps it is a result of a deficiency in our use of ESI as a source for clusters. A key question here is, essentially, How different are organic acids from inorganic acids, qualitatively, in the context of NPF? Can what we have learned about the proton transfer and hydrogen-bonding interactions of inorganic acids be straightforwardly translated to organic acids, or do the constraints of sterics and hydrophobic interactions change things significantly? The exploration of additional inorganic acids will be important as well, particularly for acids that feature new intermolecular interactions. In particular, clusters of iodic acid are likely to show some competition between halogen bonding, proton transfer, and hydrogen bonding, as well as the possibility for additional covalent chemistry involving the production of I_2O_5. Similarly, the influence of biomolecules is beginning to be explored and offers fruitful avenues for study.

7.2. Spectroscopy of Size- or Mass-Selected Neutral Clusters

Thus far, most of the spectroscopic study of these clusters has been by techniques that incorporate mass spectrometry, limiting them to ionic clusters. However, this does not necessarily have to be the case—techniques exist that permit the spectroscopy of neutral clusters, some with nearly the same amount of compositional precision as mass spectrometry–based methods. Even the most sensitive direct absorption spectroscopy techniques require sample densities several orders of magnitude higher than those in ambient NPF events. However, it is possible to perform direct spectroscopy measurements on nucleating particles in flows of gasses such as CO_2 and alkanes expanding through nozzles. Given careful consideration of the kinetics and thermodynamics of formation and growth, such experiments on NPF-relevant vapors are likely to yield insights into the cluster-particle transition that would be difficult in mass-selective experiments.

At the smaller size range, helium nanodroplet–based spectroscopy experiments offer a straightforward approach to forming and spectroscopically interrogating relatively complex neutral clusters. Here, ultracold helium droplets pick up vapors sequentially to form ultracold clusters that can be interrogated spectroscopically, similarly to the action spectroscopy techniques discussed above. If neutral clusters can be formed in the gas phase without the need for droplets, then IR/photoionization double resonance techniques can be used as well. Both of these approaches give compositional information by mass spectrometry after spectroscopy, so it is possible that weakly bound molecules will evaporate during the ionization process, but the benefit of being able to study neutrals, for which a wealth of quantum chemical studies exist for comparison, far outweighs this drawback. Moving away from action-based techniques, the deposition of mass-selected clusters, perhaps charge balanced by codeposition with oppositely charged vapors, into frozen matrices makes possible matrix isolation FTIR on reasonably mass-selected clusters.

Finally, one can imagine that action spectroscopy in the sampling interface of a cluster mass spectrometer (such as ones used in field campaigns) prior to ionization could produce sufficient dissociation to measurably change the detected mass spectrum. Deconvolution of the changes of the full mass spectrum ought to yield a size- and roughly composition-dependent mass spectrum of neutral clusters. Notably, such an approach is likely the best way to achieve a field-portable spectrometer capable of recording IR or UV/visible spectra of clusters sampled directly from the ambient atmosphere.

8. SUMMARY

Laboratory-based spectroscopic studies of clusters with compositions relevant to NPF provide molecular-level insights into the intermolecular interactions governing the mechanism of particle formation and growth. They also generate precise experimental benchmarks for theoretical studies, particularly for difficult computational searches to find global minimum energy structures.

Annu. Rev. Phys. Chem. 2023.74:99-121. Downloaded from www.annualreviews.org
Access provided by State University of New York - Stony Brook on 10/24/23. See copyright for approved use.

We have shown how spectroscopic investigations have revealed unintuitive acid-base interactions in small clusters consisting of known NPF-accelerating vapors, elucidated the structures of ever-larger clusters, and explored the complex PESs of cluster hydrates. We have also discussed efforts to extend spectroscopic insights beyond the size range in which determination of the absolute cluster structure is feasible and extensions of these studies to emerging vapors of importance in NPF, critical neutral clusters, and even the potential to apply such measurements to ambiently sampled particles in the field. Given the timeliness of climate challenges and the importance of accurate treatment of NPF in climate models, we hope that these studies serve as a foundation for further unraveling this complex process.

DISCLOSURE STATEMENT

The authors are not aware of any affiliations, memberships, funding, or financial holdings that might be perceived as affecting the objectivity of this review.

ACKNOWLEDGMENTS

The authors thank Hanna Vehkamaki, Nanna Myllys, and Monica Passananti for helpful discussions about new particle formation (NPF) and Knut Asmis, Xue-Bin Wang, and Jer-Lai Kuo for helpful discussions about the spectroscopy of NPF-relevant clusters. This material is based upon work supported by the National Science Foundation (grants CHE-1137404, CHE-1566019, and CHE-1905172).

LITERATURE CITED

1. Seinfeld J. 2003. Tropospheric chemistry and composition—aerosols/particles. In *Encyclopedia of Atmospheric Sciences*, ed. JR Holton, pp. 2349–54. New York: Academic
2. IPCC. 2013. *Climate Change 2013: The Physical Science Basis. Contribution of Working Group I to the Fifth Assessment Report of the Intergovernmental Panel on Climate Change*, ed. RK Pachauri, LA Meyer. Geneva, Switz.: IPCC
3. Marcolli C, Krieger UK. 2020. Relevance of particle morphology for atmospheric aerosol processing. *Trends Chem.* 2(1):1–3
4. Zhang R. 2010. Getting to the critical nucleus of aerosol formation. *Science* 328(5984):1366–67
5. Lee SH, Gordon H, Yu H, Lehtipalo K, Haley R, et al. 2019. New particle formation in the atmosphere: from molecular clusters to global climate. *J. Geophys. Res. Atmos.* 124(13):7098–146
6. Yu F. 2006. Effect of ammonia on new particle formation: a kinetic H_2SO_4-H_2O-NH_3 nucleation model constrained by laboratory measurements. *J. Geophys. Res. Atmos.* 111(D1):D01204
7. Gordon H, Kirkby J, Baltensperger U, Bianchi F, Breitenlechner M, et al. 2017. Causes and importance of new particle formation in the present-day and preindustrial atmospheres. *J. Geophys. Res. Atmos.* 122(16):8739–60
8. Wang M, Kong W, Marten R, He XC, Chen D, et al. 2020. Rapid growth of new atmospheric particles by nitric acid and ammonia condensation. *Nature* 581(7807):184–89
9. Baccarini A, Karlsson L, Dommen J, Duplessis P, Vüllers J, et al. 2020. Frequent new particle formation over the high Arctic pack ice by enhanced iodine emissions. *Nat. Commun.* 11(1):4924
10. Olenius T, Halonen R, Kurtén T, Henschel H, Kupiainen-Määttä O, et al. 2017. New particle formation from sulfuric acid and amines: comparison of monomethylamine, dimethylamine, and trimethylamine. *J. Geophys. Res. Atmos.* 122(13):7103–18
11. Elm J, Passananti M, Kurtén T, Vehkamäki H. 2017. Diamines can initiate new particle formation in the atmosphere. *J. Phys. Chem. A* 121(32):6155–64
12. Dawson ML, Varner ME, Perraud V, Ezell MJ, Gerber RB, Finlayson-Pitts BJ. 2012. Simplified mechanism for new particle formation from methanesulfonic acid, amines, and water via experiments and ab initio calculations. *PNAS* 109(46):18719–24

Annu. Rev. Phys. Chem. 2023.74:99-121. Downloaded from www.annualreviews.org
Access provided by State University of New York - Stony Brook on 10/24/23. See copyright for approved use.

13. Kürten A, Li C, Bianchi F, Curtius J, Dias A, et al. 2018. New particle formation in the sulfuric acid–dimethylamine–water system: reevaluation of CLOUD chamber measurements and comparison to an aerosol nucleation and growth model. *Atmos. Chem. Phys.* 18:845–63
14. Wagner R, Yan C, Lehtipalo K, Duplissy J, Nieminen T, et al. 2017. The role of ions in new particle formation in the CLOUD chamber. *Atmos. Chem. Phys.* 17(24):15181–97
15. Karthika S, Radhakrishnan TK, Kalaichelvi P. 2016. A review of classical and nonclassical nucleation theories. *Cryst. Growth Des.* 16(11):6663–81
16. Laaksonen A. 2000. Application of nucleation theories to atmospheric aerosol formation. *AIP Conf. Proc.* 534:711–23
17. McGrath MJ, Olenius T, Ortega IK, Loukonen V, Paasonen P, et al. 2012. Atmospheric Cluster Dynamics Code: a flexible method for solution of the birth-death equations. *Atmos. Chem. Phys.* 12(5):2345–55
18. Elm J. 2019. An atmospheric cluster database consisting of sulfuric acid, bases, organics, and water. *ACS Omega* 4:10965–74
19. Almeida J, Schobesberger S, Kürten A, Ortega IK, Kupiainen-Määttä O, et al. 2013. Molecular understanding of sulphuric acid–amine particle nucleation in the atmosphere. *Nature* 502:359–63
20. Kubečka J, Besel V, Kurtén T, Myllys N, Vehkamäki H. 2019. Configurational sampling of noncovalent (atmospheric) molecular clusters: sulfuric acid and guanidine. *J. Phys. Chem. A* 123(28):6022–33
21. Kurfman LA, Odbadrakh TT, Shields GC. 2021. Calculating reliable Gibbs free energies for formation of gas-phase clusters that are critical for atmospheric chemistry: $(H_2SO_4)_3$. *J. Phys. Chem. A* 125(15):3169–76
22. Henschel H, Navarro JCA, Yli-Juuti T, Kupiainen-Määttä O, Olenius T, et al. 2014. Hydration of atmospherically relevant molecular clusters: computational chemistry and classical thermodynamics. *J. Phys. Chem. A* 118(14):2599–611
23. Kulmala M. 2003. How particles nucleate and grow. *Science* 302(5647):1000–1
24. Kalkavouras P, Bougiatioti A, Kalivitis N, Stavroulas I, Tombrou M, et al. 2019. Regional new particle formation as modulators of cloud condensation nuclei and cloud droplet number in the eastern Mediterranean. *Atmos. Chem. Phys.* 19(9):6185–203
25. Arnold F, Fabian R. 1980. First measurements of gas phase sulphuric acid in the stratosphere. *Nature* 283(5742):55–57
26. Wang S, Zordan CA, Johnston MV. 2006. Chemical characterization of individual, airborne sub-10-nm particles and molecules. *Anal. Chem.* 78(6):1750–54
27. Smith JN, Barsanti KC, Friedli HR, Ehn M, Kulmala M, et al. 2010. Observations of aminium salts in atmospheric nanoparticles and possible climatic implications. *PNAS* 107(15):6634–39
28. Sipilä M, Sarnela N, Jokinen T, Henschel H, Junninen H, et al. 2016. Molecular-scale evidence of aerosol particle formation via sequential addition of HIO_3. *Nature* 537(7621):532–34
29. Passananti M, Zapadinsky E, Zanca T, Kangasluoma J, Myllys N, et al. 2019. How well can we predict cluster fragmentation inside a mass spectrometer? *Chem. Commun.* 55(42):5946–49
30. Jen CN, McMurry PH, Hanson DR. 2014. Stabilization of sulfuric acid dimers by ammonia, methylamine, dimethylamine, and trimethylamine. *J. Geophys. Res. Atmos.* 119:7502–14
31. Kirkby J, Curtius J, Almeida J, Dunne E, Duplissy J, et al. 2011. Role of sulphuric acid, ammonia and galactic cosmic rays in atmospheric aerosol nucleation. *Nature* 476(7361):429–33
32. Kürten A, Bianchi F, Almeida J, Kupiainen-Määttä O, Dunne EM, et al. 2016. Experimental particle formation rates spanning tropospheric sulfuric acid and ammonia abundances, ion production rates, and temperatures. *J. Geophys. Res. Atmos.* 121(20):12377–400
33. Waller SE, Yang Y, Castracane E, Kreinbihl JJ, Nickson KA, Johnson CJ. 2019. Electrospray ionization-based synthesis and validation of amine-sulfuric acid clusters of relevance to atmospheric new particle formation. *J. Am. Soc. Mass Spectrom.* 30:2267–77
34. Thomas JM, He S, Larriba-Andaluz C, DePalma JW, Johnston MV, Hogan CJ Jr. 2016. Ion mobility spectrometry-mass spectrometry examination of the structures, stabilities, and extents of hydration of dimethylamine–sulfuric acid clusters. *Phys. Chem. Chem. Phys.* 18:22962–72
35. Gerlich D. 1992. *Inhomogeneous RF Fields: A Versatile Tool for the Study of Processes with Slow Ions*. Hoboken, NJ: Wiley
36. Froyd KD, Lovejoy ER. 2011. Bond energies and structures of ammonia–sulfuric acid positive cluster ions. *J. Phys. Chem. A* 116(24):5886–99

Annu. Rev. Phys. Chem. 2023.74:99-121. Downloaded from www.annualreviews.org
Access provided by State University of New York - Stony Brook on 10/24/23. See copyright for approved use.

Annu. Rev. Phys. Chem. 2023.74:99-121. Downloaded from www.annualreviews.org
Access provided by State University of New York - Stony Brook on 10/24/23. See copyright for approved use.

37. Maier-Borst M, Cameron DB, Rokni M, Parks JH. 1999. Electron diffraction of trapped cluster ions. *Phys. Rev. A* 59(5):R3162–65
38. Ekeberg T, Svenda M, Abergel C, Maia FRNC, Seltzer V, et al. 2015. Three-dimensional reconstruction of the giant mimivirus particle with an x-ray free-electron laser. *Phys. Rev. Lett.* 114(9):098102
39. Polfer NC. 2011. Infrared multiple photon dissociation spectroscopy of trapped ions. *Chem. Soc. Rev.* 40(5):2211–21
40. Wolk AB, Leavitt CM, Garand E, Johnson MA. 2014. Cryogenic ion chemistry and spectroscopy. *Acc. Chem. Res.* 47(1):202–10
41. Yuan Q, Cao W, Wang XB. 2020. Cryogenic and temperature-dependent photoelectron spectroscopy of metal complexes. *Int. Rev. Phys. Chem.* 39(1):83–108
42. Bene JED, Jordan MJT. 1999. Vibrational spectroscopy of the hydrogen bond: an ab initio quantum-chemical perspective. *Int. Rev. Phys. Chem.* 18(1):119–62
43. Johnson CJ, Dzugan LC, Wolk AB, Leavitt CM, Fournier JA, et al. 2014. Microhydration of contact ion pairs in $M^{2+}OH^-(H_2O)_{n=1-5}$ (M = Mg, Ca) clusters: spectral manifestations of a mobile proton defect in the first hydration shell. *J. Phys. Chem. A* 118(35):7590–97
44. Mishra S, Nguyen HQ, Huang QR, Lin CK, Kuo JL, Patwari GN. 2020. Vibrational spectroscopic signatures of hydrogen bond induced NH stretch–bend Fermi-resonance in amines: the methylamine clusters and other N–H···N hydrogen-bonded complexes. *J. Chem. Phys.* 153(19):194301
45. DePalma JW, Bzdek BR, Doren DJ, Johnston MV. 2012. Structure and energetics of nanometer size clusters of sulfuric acid with ammonia and dimethylamine. *J. Phys. Chem. A* 116:1030–40
46. Kupiainen O, Ortega I, Kurtén T, Vehkamäki H. 2012. Amine substitution into sulfuric acid–ammonia clusters. *Atmos. Chem. Phys.* 12(8):3591–99
47. Johnson CJ, Johnson MA. 2013. Vibrational spectra and fragmentation pathways of size-selected, D_2-tagged ammonium/methylammonium bisulfate clusters. *J. Phys. Chem. A* 117(50):13265–74
48. Kreinbihl JJ, Frederiks NC, Waller SE, Yang Y, Johnson CJ. 2020. Establishing the structural motifs present in small ammonium and aminium bisulfate clusters of relevance to atmospheric new particle formation. *J. Chem. Phys.* 153(3):034307
49. Yacovitch TI, Heine N, Brieger C, Wende T, Hock C, et al. 2013. Vibrational spectroscopy of bisulfate/sulfuric acid/water clusters: structure, stability, and infrared multiple-photon dissociation intensities. *J. Phys. Chem. A* 117(32):7081–90
50. Yacovitch TI, Heine N, Brieger C, Wende T, Hock C, et al. 2012. Vibrational spectroscopy of atmospherically relevant acid cluster anions: bisulfate versus nitrate core structures. *J. Chem. Phys.* 136(24):241102
51. Hou GL, Wang XB, Valiev M. 2017. Formation of $(HCOO^-)(H_2SO_4)$ anion clusters: violation of gas-phase acidity predictions. *J. Am. Chem. Soc.* 139(33):11321–24
52. Hou GL, Valiev M, Wang XB. 2019. Sulfuric acid and aromatic carboxylate clusters $H_2SO_4{\cdot}ArCOO^-$: structures, properties, and their relevance to the initial aerosol nucleation. *Int. J. Mass Spectrom.* 439:27–33
53. Hou GL, Lin W, Deng S, Zhang J, Zheng WJ, et al. 2013. Negative ion photoelectron spectroscopy reveals thermodynamic advantage of organic acids in facilitating formation of bisulfate ion clusters: atmospheric implications. *J. Phys. Chem. Lett.* 4(5):779–85
54. Hou GL, Valiev M, Wang XB. 2016. Deprotonated dicarboxylic acid homodimers: hydrogen bonds and atmospheric implications. *J. Phys. Chem. A* 120(15):2342–49
55. Waller SE, Yang Y, Castracane E, Racow EE, Kreinbihl JJ, et al. 2018. The interplay between hydrogen bonding and Coulombic forces in determining the structure of sulfuric acid-amine clusters. *J. Phys. Chem. Lett.* 9(6):1216–22
56. Fatila EM, Twum EB, Sengupta A, Pink M, Karty JA, et al. 2016. Anions stabilize each other inside macrocyclic hosts. *Angew. Chem. Int. Ed.* 55(45):14057–62
57. Hou GL, Lin W, Wang XB. 2018. Direct observation of hierarchic molecular interactions critical to biogenic aerosol formation. *Commun. Chem.* 1:37
58. Ehn M, Junninen H, Petäjä T, Kurtén T, Kerminen VM, et al. 2010. Composition and temporal behavior of ambient ions in the boreal forest. *Atmos. Chem. Phys.* 10(17):8513–30

Annu. Rev. Phys. Chem. 2023.74:99-121. Downloaded from www.annualreviews.org
Access provided by State University of New York - Stony Brook on 10/24/23. See copyright for approved use.

59. Schobesberger S, Junninen H, Bianchi F, Lönn G, Ehn M, et al. 2013. Molecular understanding of atmospheric particle formation from sulfuric acid and large oxidized organic molecules. *PNAS* 110(43):17223–28
60. Lehtipalo K, Yan C, Dada L, Bianchi F, Xiao M, et al. 2018. Multicomponent new particle formation from sulfuric acid, ammonia, and biogenic vapors. *Sci. Adv.* 4(12):eaau5363
61. Carl DR, Armentrout PB. 2013. Threshold collision-induced dissociation of hydrated magnesium: experimental and theoretical investigation of the binding energies for $Mg^{2+}(H_2O)_x$ complexes ($x = 2$–10). *Chem. Phys. Chem.* 14(4):681–97
62. Yeh L, Okumura M, Myers J, Price J, Lee Y. 1989. Vibrational spectroscopy of the hydrated hydronium cluster ions $H_3O^+(H_2O)_n$ ($n = 1, 2, 3$). *J. Chem. Phys.* 91(12):7319–30
63. Wang YS, Chang HC, Jiang JC, Lin SH, Lee YT, Chang HC. 1998. Structures and isomeric transitions of NH_4^+ $(H_2O)_{3–6}$: from single to double rings. *J. Am. Chem. Soc.* 120(34):8777–88
64. Serxner D, Dessent CE, Johnson MA. 1996. Precursor of the I^-_{aq} charge-transfer-to-solvent (CTTS) band in $I^-(H_2O)_n$ clusters. *J. Chem. Phys.* 105(16):7231–34
65. Goebbert DJ, Garand E, Wende T, Bergmann R, Meijer G, et al. 2009. Infrared spectroscopy of the microhydrated nitrate ions NO_3^- $(H_2O)_{1–6}$. *J. Phys. Chem. A* 113(26):7584–92
66. Heine N, Kratz EG, Bergmann R, Schofield DP, Asmis KR, et al. 2014. Vibrational spectroscopy of the water–nitrate complex in the O–H stretching region. *J. Phys. Chem. A* 118(37):8188–97
67. Wang XB, Yang X, Wang LS, Nicholas JB. 2002. Photodetachment and theoretical study of free and water-solvated nitrate anions, NO_3^- $(H_2O)_n$ ($n = 0$–6). *J. Chem. Phys.* 116(2):561–70
68. Wang XB, Nicholas JB, Wang LS. 2000. Electronic instability of isolated SO_4^{2-} and its solvation stabilization. *J. Chem. Phys.* 113(24):10837–40
69. Zhou J, Santambrogio G, Brümmer M, Moore DT, Wöste L, et al. 2006. Infrared spectroscopy of hydrated sulfate dianions. *J. Chem. Phys.* 125(11):111102
70. Wang XB, Sergeeva AP, Yang J, Xing XP, Boldyrev AI, Wang LS. 2009. Photoelectron spectroscopy of cold hydrated sulfate clusters, SO_4^{2-} $(H_2O)_n$ ($n = 4$–7): temperature-dependent isomer populations. *J. Phys. Chem. A* 113(19):5567–76
71. Yacovitch TI, Wende T, Jiang L, Heine N, Meijer G, et al. 2011. Infrared spectroscopy of hydrated bisulfate anion clusters: $HSO_4^-(H_2O)_{1–16}$. *J. Phys. Chem. Lett.* 2(17):2135–40
72. Hou GL, Zhang J, Valiev M, Wang XB. 2017. Structures and energetics of hydrated deprotonated *cis*-pinonic acid anion clusters and their atmospheric relevance. *Phys. Chem. Chem. Phys.* 19(16):10676–84
73. Hou GL, Kong XT, Valiev M, Jiang L, Wang XB. 2016. Probing the early stages of solvation of *cis*-pinate dianions by water, acetonitrile, and methanol: a photoelectron spectroscopy and theoretical study. *Phys. Chem. Chem. Phys.* 18(5):3628–37
74. Wanko M, Wende T, Saralegui MM, Jiang L, Rubio A, Asmis KR. 2013. Solvent-mediated folding of dicarboxylate dianions: aliphatic chain length dependence and origin of the IR intensity quenching. *Phys. Chem. Chem. Phys.* 15(47):20463–72
75. Heine N, Yacovitch TI, Schubert F, Brieger C, Neumark DM, Asmis KR. 2014. Infrared photodissociation spectroscopy of microhydrated nitrate–nitric acid clusters NO_3^- $(HNO_3)_m$ $(H_2O)_n$. *J. Phys. Chem. A* 118(35):7613–22
76. McCaslin LM, Johnson MA, Gerber RB. 2019. Mechanisms and competition of halide substitution and hydrolysis in reactions of N_2O_5 with seawater. *Sci. Adv.* 5(6):eaav6503
77. DePalma JW, Kelleher PJ, Johnson CJ, Fournier JA, Johnson MA. 2015. Vibrational signatures of solvent-mediated deformation of the ternary core ion in size-selected $[MgSO_4Mg(H_2O)_{n=4–11}]^{2+}$ clusters. *J. Phys. Chem. A* 119(30):8294–302
78. Jiang L, Wende T, Bergmann R, Meijer G, Asmis KR. 2010. Gas-phase vibrational spectroscopy of microhydrated magnesium nitrate ions $[MgNO_3$ $(H_2O)_{1–4}]^+$. *J. Am. Chem. Soc.* 132(21):7398–404
79. Wende T, Heine N, Yacovitch TI, Asmis KR, Neumark DM, Jiang L. 2016. Probing the microsolvation of a quaternary ion complex: gas phase vibrational spectroscopy of $(NaSO_4^-)_2$ $(H_2O)_{n=0–6,8}$. *Phys. Chem. Chem. Phys.* 18(1):267–77
80. Kreinbihl JJ, Frederiks NC, Johnson CJ. 2021. Hydration motifs of ammonium bisulfate clusters show complex temperature dependence. *J. Chem. Phys.* 154(1):014304

81. Yang Y, Johnson CJ. 2019. Hydration motifs of ammonium bisulfate clusters of relevance to atmospheric new particle formation. *Faraday Discuss.* 217:47–66
82. Thomas JM, He S, Larriba-Andaluz C, DePalma JW, Johnston MV, Hogan CJ Jr. 2016. Ion mobility spectrometry-mass spectrometry examination of the structures, stabilities, and extents of hydration of dimethylamine–sulfuric acid clusters. *Phys. Chem. Chem. Phys.* 18:22962–72
83. Yang Y, Waller SE, Kreinbihl JJ, Johnson CJ. 2018. Direct link between structure and hydration in ammonium and aminium bisulfate clusters implicated in atmospheric new particle formation. *J. Phys. Chem. Lett.* 9(18):5647–52
84. Tsona NT, Henschel H, Bork N, Loukonen V, Vehkamäki H. 2015. Structures, hydration, and electrical mobilities of bisulfate ion–sulfuric acid–ammonia/dimethylamine clusters: a computational study. *J. Phys. Chem. A* 119:9670–79
85. Rozenberg M, Loewenschuss A. 2009. Matrix isolation infrared spectrum of the sulfuric acid–monohydrate complex: new assignments and resolution of the "missing H-bonded ν (OH) band" issue. *J. Phys. Chem. A* 113(17):4963–71
86. Rozenberg M, Loewenschuss A, Nielsen CJ. 2011. Complexes of molecular and ionic character in the same matrix layer: infrared studies of the sulfuric acid/ammonia system. *J. Phys. Chem. A* 115(23):5759–66
87. Rozenberg M, Loewenschuss A, Nielsen CJ. 2016. H-bonding of sulfuric acid with its decomposition products: an infrared matrix isolation and computational study of the $H_2SO_4{\cdot}H_2O{\cdot}SO_3$ complex. *J. Phys. Chem. A* 120(20):3450–55
88. Rozenberg M, Loewenschuss A, Nielsen CJ. 2014. Trimethylamine/sulfuric acid/water clusters: a matrix isolation infrared study. *J. Phys. Chem. A* 118(6):1004–11
89. Rozenberg M, Loewenschuss A, Nielsen CJ. 2015. H-bonding of formic acid with its decomposition products: a matrix isolation and computational study of the HCOOH/CO and HCOOH/CO_2 complexes. *J. Phys. Chem. A* 119(31):8497–502
90. Haupa K, Bil A, Barnes A, Mielke Z. 2015. Isomers of the acetic acid–water complex trapped in an argon matrix. *J. Phys. Chem. A* 119(11):2522–31
91. Cziczo DJ, Abbatt JPD. 2000. Infrared observations of the response of NaCl, $MgCl_2$, NH_4HSO_4, and NH_4NO_3 aerosols to changes in relative humidity from 298 to 238 K. *J. Phys. Chem. A* 104(10):2038–47
92. Gao X, Zhang Y, Liu Y. 2018. Temperature-dependent hygroscopic behaviors of atmospherically relevant water-soluble carboxylic acid salts studied by ATR-FTIR spectroscopy. *Atmos. Environ.* 191:312–19
93. Kelleher PJ, Menges FS, DePalma JW, Denton JK, Johnson MA, et al. 2017. Trapping and structural characterization of the $XNO_2{\cdot}NO_3^-$ (X = Cl, Br, I) exit channel complexes in the water-mediated X^- + N_2O_5 reactions with cryogenic vibrational spectroscopy. *J. Phys. Chem. Lett.* 8(19):4710–15
94. Lee AK, Ling T, Chan CK. 2008. Understanding hygroscopic growth and phase transformation of aerosols using single particle Raman spectroscopy in an electrodynamic balance. *Faraday Discuss.* 137:245–63
95. Birdsall AW, Krieger UK, Keutsch FN. 2018. Electrodynamic balance–mass spectrometry of single particles as a new platform for atmospheric chemistry research. *Atmos. Meas. Tech.* 11(1):33–47
96. Esser TK, Hoffmann B, Anderson SL, Asmis KR. 2019. A cryogenic single nanoparticle action spectrometer. *Rev. Sci. Instrum.* 90(12):125110

Annu. Rev. Phys. Chem. 2023.74:99-121. Downloaded from www.annualreviews.org
Access provided by State University of New York - Stony Brook on 10/24/23. See copyright for approved use.

Annual Review of
Physical Chemistry
Volume 74, 2023

Contents

Annu. Rev. Phys. Chem. 2023.74:99-121. Downloaded from www.annualreviews.org
Access provided by State University of New York - Stony Brook on 10/24/23. See copyright for approved use.

Annu. Rev. Phys. Chem. 2023.74:99-121. Downloaded from www.annualreviews.org
Access provided by State University of New York - Stony Brook on 10/24/23. See copyright for approved use.

Errata

An online log of corrections to *Annual Review of Physical Chemistry* articles may be found at http://www.annualreviews.org/errata/physchem

Annu. Rev. Phys. Chem. 2023.74:99-121. Downloaded from www.annualreviews.org
Access provided by State University of New York - Stony Brook on 10/24/23. See copyright for approved use.